

A Study of Silver (I) Ion–Organonitrile Complexes: Ion Structures, Binding Energies, and Substituent Effects

Tamer Shoeib, Houssain El Aribi, K. W. Michael Siu, and Alan C. Hopkinson*

Department of Chemistry and Centre for Research in Mass Spectrometry, York University,
Toronto, Ontario M3J 1P3, Canada

Received: July 26, 2000; In Final Form: October 27, 2000

Density functional calculations at B3LYP/DZVP are used to obtain the binding enthalpies and free energies for the reaction $\text{Ag}^+ + \text{XCN} \rightarrow \text{AgNCX}^+$, where $\text{X} = \text{H}, \text{CH}_3, \text{NH}_2, \text{OH}, \text{F}, \text{CF}_3, \text{CN}, \text{NO}_2, \text{N}(\text{CH}_3)_2, \text{C}_6\text{H}_5, p\text{-C}_6\text{H}_4\text{N}(\text{CH}_3)_2, p\text{-C}_6\text{H}_4\text{NO}_2, \text{ and } p\text{-C}_6\text{H}_4\text{NH}_2$. The calculated binding enthalpies at 298 K range from 52.2 kcal mol⁻¹ for $\text{X} = p\text{-C}_6\text{H}_4\text{N}(\text{CH}_3)_2$ to 21.3 kcal mol⁻¹ for $\text{X} = \text{NO}_2$. Calculations at this level of theory are also used to optimize the structures of $\text{Ag}(\text{NCCH}_3)_n^+$ and $\text{Ag}(\text{NCH})_n^+$ ions, where $n = 1\text{--}6$. The binding enthalpies for the addition of the first and second molecules of CH_3CN are 40.1 and 35.3 kcal mol⁻¹, whereas for HCN , they are calculated to be 31.2 and 28.3 kcal mol⁻¹, respectively. The binding enthalpies of the third and fourth ligands are much smaller at 15.9 and 10.8 kcal mol⁻¹ for CH_3CN and 13.5 and 9.7 kcal mol⁻¹ for HCN . The 5- and 6-coordinate structures have positive free energies of formation with both ligands. Electrospraying a solution of AgNO_3 and acetonitrile in water shows the dominant ions to be Ag^+ , AgNCCH_3^+ , and $\text{Ag}(\text{NCCH}_3)_2^+$, with the $\text{Ag}(\text{NCCH}_3)_3^+$ ion being observed only in very small amounts and only under relatively mild conditions. Energy-resolved collision-induced dissociation (CID) experiments confirm the $\text{Ag}(\text{NCCH}_3)_3^+$ ion to be a loosely bound species, while the $\text{Ag}(\text{NCCH}_3)_2^+$ and AgNCCH_3^+ ions have substantially higher and comparable binding energies. Using the threshold method, we determined the binding energies at 0 K of NCCH_3 to Ag^+ and of NCCH_3 to AgNCCH_3^+ to be 38.7 and 34.6 kcal mol⁻¹, respectively; the corresponding energies at 298 K are 39.4 and 34.7 kcal mol⁻¹.

Introduction

The solution-phase chemistry of various transition metal ion–ligand complexes provides valuable insights into the fields of heterogeneous catalysis and organometallic reactions and furthers our understanding of the interactions of these ions with biological systems.^{1–4} Gas-phase studies, on the other hand, provide the binding energies and relative reactivities of these ions in the absence of solvent effects.^{5–23} Thermodynamic properties obtained from gas-phase studies are directly comparable with those from theoretical studies, and many gas-phase experimental studies have been successfully combined with ab initio molecular orbital calculations.^{24–31}

In the gas phase, the interactions of transition metal ions with a variety of ligands such as amines, alcohols, and carbonyl functional groups are described as electrostatic in nature.^{32–38} This relatively weak binding results in the geometry of the ligand in the complex to be largely unchanged from that of the free ligand. This is particularly well illustrated in our recent studies on Mg^+ and Ag^+ complexes with NH_3 .³⁹

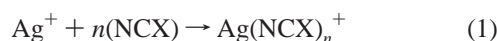
Silver (I) binds strongly to peptides.^{40–45} Fragmentations of silver–peptide complexes in the gas phase have been shown to be effective for peptide sequencing.⁴⁶ The silver ion can bind to a large number of sites on a peptide, including the amino nitrogen at the N-terminus, basic groups on the side chain, and the carbonyl oxygens of the peptide bonds.^{42–45} Recent ab initio calculations have shown Ag^+ to be mono-, di-, and tri-coordinate in complexes with α -amino acids, and tetracoordinated Ag^+ occurs in relatively small peptides. All are stable species, with

the isomers having the highest coordination number typically being the most energetically favored.⁴⁷ In larger peptides, the number of chelating sites that simultaneously interact with the silver ion generally does not exceed the number of free ligands that can coordinate to Ag^+ .

Ag^+ has a d^{10} valence shell, which is close to being saturated; however, being a large and easily polarizable metal, silver (I) may be expected to accommodate a large number of ligands in its coordination sphere. Complexes of Ag^+ with NH_3 ,⁴⁸ imidazole,⁴⁹ and pyridine⁵⁰ have been shown to be dicoordinate and linear by means of X-ray crystallography. Four-coordinate tetrahedral complexes of Ag^+ with acetonitrile⁵¹ and bipyridine derivatives, such as 4,4',6,6'-tetramethyl-2,2'-bipyridine,⁵² were observed in the solid state. In solution, di-, tri-, and tetracoordinated Ag^+ complexes with NH_3 ⁵³ and with pyrazine⁵⁴ were observed, depending on the mole ratio of the silver (I) ion to the coordinating ligand. In a wide variety of neat solvents, including water, pyridine, acetonitrile, tetramethyl phosphate, *N,N*-dimethylformamide, 1,1,3,3-tetramethylurea, dimethyl sulfide, *N*-propylamine, and 2-methylpyridine, Ag^+ was shown to have tetrahedral coordination.⁵⁵

To the best of our knowledge, complexes of Ag^+ with more than four directly coordinated ligands have never been observed experimentally. Recently, some calculations indicated that the free energies for formation of trigonal bipyramidal $\text{Ag}(\text{NCX})_5^+$ from $\text{Ag}(\text{NCX})_4^+$, where $\text{X} = \text{H}$ or CH_3 , are small but negative.⁵⁵ The enthalpy calculated by Tsutsui et al.⁵⁵ for the addition of two CH_3CN molecules to Ag^+ is 48.6 kcal mol⁻¹, which is in considerable disagreement with the value of 84.3

± 3 kcal mol⁻¹ of Deng and Kebabian,⁴² determined using high-pressure mass spectrometry. In this paper, we attempt to resolve this apparent disagreement. We report the geometries, enthalpies, and free energies of formation for the following reactions



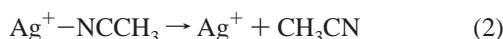
where X = H or CH₃ and $n = 1-6$. We also report the effects of varying the X groups in the nitrile on the silver (I) ion binding enthalpies for the first XCN addition as well as on the geometries of the resulting complexes.

Computational Methods. Molecular orbital calculations were performed using Gaussian 98.⁵⁶ All structures were optimized without any symmetry constraints by the density functional theory (DFT), using the B3LYP hybrid method,⁵⁷⁻⁵⁹ and the DZVP basis set.^{60,61} All critical points were characterized by harmonic frequency calculations and were shown to be at minima. Corrections for basis set superposition errors (BSSE) were made using the counterpoise method.⁶² Calculated total energies are given in Tables 1, 4, and 5.

Experimental Method. Experiments were carried out on a PE-SCIEX API III triple-quadrupole mass spectrometer (Concord, Ontario, Canada). A solution of approximately 50 μM silver nitrate in 40/20/40 (V/V/V) water/methanol/acetonitrile was introduced into the ion source at atmospheric pressure using a syringe pump (Harvard Apparatus, Model 22, South Natick, MA) at a flow rate of 5 $\mu\text{L}/\text{min}$. Silver complexes of acetonitrile were generated by means of a pneumatically assisted electrospray with air as the nebulizer gas. The ions were sampled through a dry nitrogen curtain, an orifice, and into the quadrupole q_0 operated in rf-only mode. The ions of interest were mass-selected by the first quadrupole Q_1 , injected into the second quadrupole q_2 , where they underwent collisional activation with argon atoms, resulting in dissociation, and their product ions were then mass-analyzed in a third quadrupole Q_3 and detected.

Data and Threshold Analysis. A typical Q_1 scan spectrum shows the ion $\text{Ag}(\text{NCCH}_3)^+$ to be dominant. The ion $\text{Ag}(\text{NCCH}_3)_2^+$ is also present, but at much lower abundance, while no evidence of $\text{Ag}(\text{NCCH}_3)_3^+$ was observed. Under very mild collision conditions in the lens region, the $\text{Ag}(\text{NCCH}_3)_2^+$ ion became the dominant species, with $\text{Ag}(\text{NCCH}_3)_3^+$ being at an abundance of about 5–10%.

Collision-induced dissociation (CID) of $\text{Ag}(\text{NCCH}_3)^+$ with Ar produces Ag^+



The threshold energy, E_0 of reaction 2 was determined using the curve fitting and modeling procedure CRUNCH, developed by Armentrout and co-workers.⁶³⁻⁶⁹ The product ion intensities were first converted to cross sections.⁶³⁻⁶⁹ The fitting procedure is based on the equation

$$\sigma = \sigma_0 \sum g_i (E + E_i - E_0)^n / E \quad (3)$$

where σ is the dissociation cross section, E is the kinetic energy of the silver complex ion in the center-of-mass frame, E_i is the internal vibrational energy in a given vibrational state whose probability at a given temperature is g_i (if $\sum g_i = 1$, the summation is over the ro-vibrational states of the reactant ions), E_0 is the threshold energy and corresponds to the energy required

for the dissociation reaction at 0 K, σ_0 is an energy-independent scaling factor, and n is an adjustable parameter.

Equation 3 is only applicable to products formed as result of single collisions. In the present experiments, the Ar is being continuously monitored with an upstream Baratron gauge. The pressure is expressed as collision-gas thickness (CGT)⁷⁰ and is typically maintained between 25 and 100 $\times 10^{12}$ atoms/cm². To eliminate the effect of multiple collisions, we obtained E_0 from threshold curves constructed only from σ at zero CGT. These cross sections were obtained by extrapolating the data to zero CGT. Typically, a threshold curve comprises 120 cross section values over an E range of 0–3 eV.

In this present work, we also consider the possibility that collisionally activated complex ions do not dissociate on the time scale of the experiment. This results in a shift of the observed threshold to higher energy, the kinetic shift, a consequence of the fact that only those ions that dissociate within q_2 are observed. The magnitude of the kinetic shift is subtracted by incorporating the Rice–Ramsperger–Kassel–Marcus (RRKM) theory,⁷¹⁻⁷³ which models the unimolecular dissociation rate, into reaction 2. This requires sets of vibrational frequencies and rotational constants provided by the DFT hybrid method at the B3LYP/DZVP level of theory for both the silver complex ions and the dissociation products. (Tables 1s and 2s in the Supporting Information section list the vibrational frequencies and rotational constants.)

The upper limit to the kinetic shift is provided by a highly ordered, “tight” transition state (TS) similar in structure to the silver complex ion. Here, the parameters of the TS are assumed to be represented by those of the silver complex ion minus the single mode that corresponds to the reaction coordinate (RC) associated with the Ag–N stretching mode. This tight TS is characterized by a negative entropy of activation (ΔS^\ddagger). More appropriately, the dissociation of the silver complex is a simple bond cleavage whose TS is expected to be less ordered than that of the silver complex ion. In this case, the “loose” TS vibrational frequencies can be modeled by those of the neutral products; furthermore, the transitional frequencies, the ones that become rotations of the completely dissociated products, are treated as rotors, a treatment that corresponds to a phase space limit (PSL).^{68,69} The TS is assumed to be variationally located at the centrifugal barrier, and the adiabatic 2D rotational energy is calculated using the statistical average approach detailed by Rodgers et al.⁶⁸

Equation 3 was used to model and to analyze the threshold energies of reactions 2 and 4



Results and Discussion

Structural Features. The structures of the directly coordinated complexes $\text{Ag}(\text{NCX})_n^+$, where X = H or CH₃ and $n = 1-6$, are given in Figures 1 and 2. Total electronic energies are given in Table 1. The symmetries assigned to ions 4–6 are with regard to heavy atoms only (see Figure 1), while the symmetries of ions 1–3 and 7–12 (see Figures 1 and 2) are for the whole structures.

In general, the Ag–N distance increases monotonically with increasing number of ligands, n , in both the $\text{Ag}(\text{NCH})_n^+$ and $\text{Ag}(\text{NCCH}_3)_n^+$ series of complexes. The dicoordinated complexes in both series are, however, the exception in that the silver nitrogen distances are shorter than those of the corresponding monocoordinated species. This same trend was also

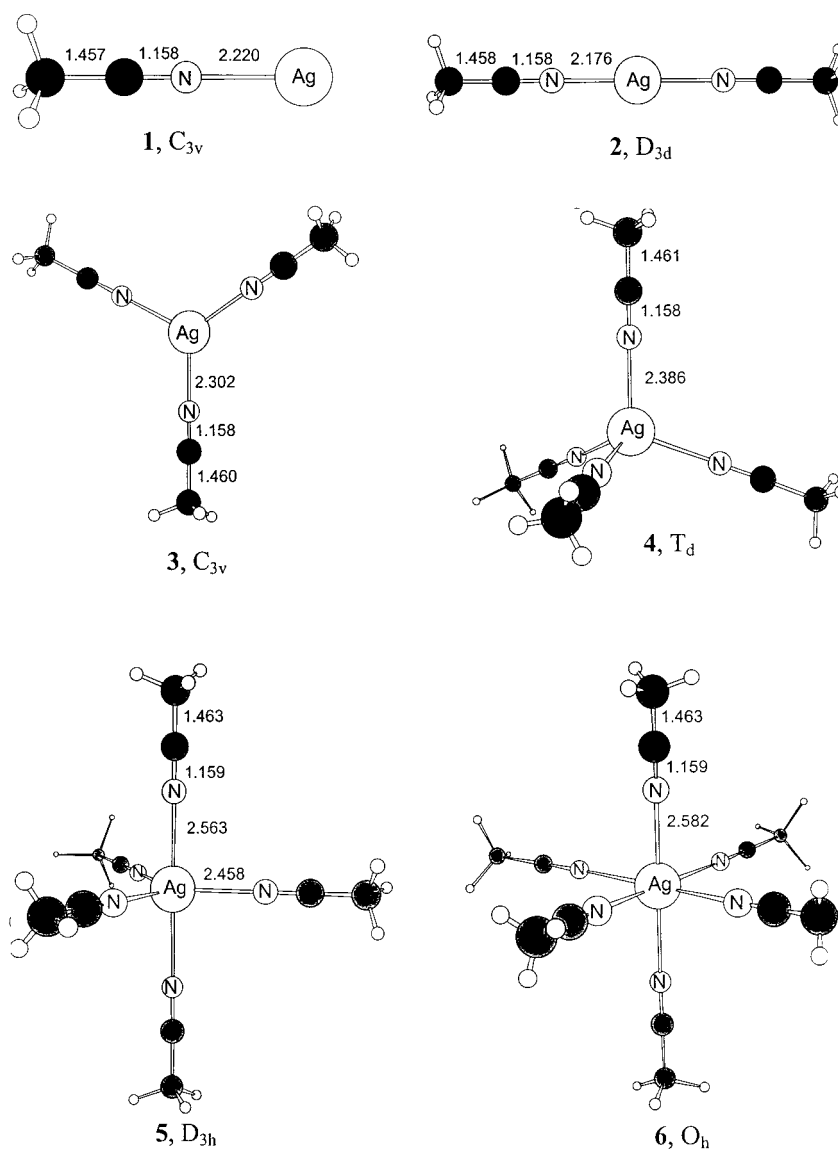


Figure 1. Structures of $\text{Ag}(\text{CH}_3\text{CN})_n^+$ ($n = 1-6$) for directly coordinated complexes, as optimized at B3LYP/DZVP. Bond lengths are in Å.

TABLE 1: Total Electronic, Unscaled Zero-Point, and Thermal Energies as well as Entropies Calculated at B3LYP/DZVP

structure number	ion/molecule	energy (Hartrees)	ZPE (kcal mol ⁻¹)	$H_{298}^\circ - H_0^\circ$ (kcal mol ⁻¹)	entropy (cal K ⁻¹ mol ⁻¹)
1	$\text{Ag}(\text{NCCH}_3)^+$	-5332.03381	29.1	4.2	77.6
2	$\text{Ag}(\text{NCCH}_3)_2^+$	-5464.86409	58.5	7.5	111.5
3	$\text{Ag}(\text{NCCH}_3)_3^+$	-5597.66226	87.5	11.1	148.9
4	$\text{Ag}(\text{NCCH}_3)_4^+$	-5730.45254	116.5	14.7	184.2
5	$\text{Ag}(\text{NCCH}_3)_5^+$	-5863.23086	145.3	17.9	215.8
6	$\text{Ag}(\text{NCCH}_3)_6^+$	-5996.00605	174.1	22.2	259.0
7	$\text{Ag}(\text{NCH})^+$	-5292.68632	10.9	3.2	57.8
8	$\text{Ag}(\text{NCH})_2^+$	-5386.17226	22.3	5.4	79.7
9	$\text{Ag}(\text{NCH})_3^+$	-5479.63379	33.4	7.7	110.6
10	$\text{Ag}(\text{NCH})_4^+$	-5573.08899	44.0	10.4	137.0
11	$\text{Ag}(\text{NCH})_5^+$	-5666.53432	54.8	13.0	157.5
12	$\text{Ag}(\text{NCH})_6^+$	-5759.97736	65.4	15.6	180.2
	HCN	-93.43350	9.1	2.4	36.7
	CH_3CN	-132.76885	28.5	3.4	60.3
	Ag^+	-5199.19815	—	1.5	39.9

observed for the addition of NH_3 molecules to Ag^+ .³⁹ The geometries of the ligands of all Ag^+ complexes studied here are relatively unchanged from those of the free ligands. This is characteristic of complexes in which the interactions between the ligands and the silver (I) ion are essentially electrostatic in nature.

Energetics. $\text{Ag}(\text{NCH})_n^+$ and $\text{Ag}(\text{NCCH}_3)_n^+$ ($n = 1-6$) Complexes. Total electronic, unscaled zero-point, and thermal energies as well as entropies for HCN, CH_3CN , Ag^+ , and $\text{Ag}(\text{NCX})_n^+$ ($n = 1-6$, X = H or CH_3), are given in Table 1. The calculated binding enthalpies and free energies for direct coordination of up to six HCN and CH_3CN molecules with Ag^+

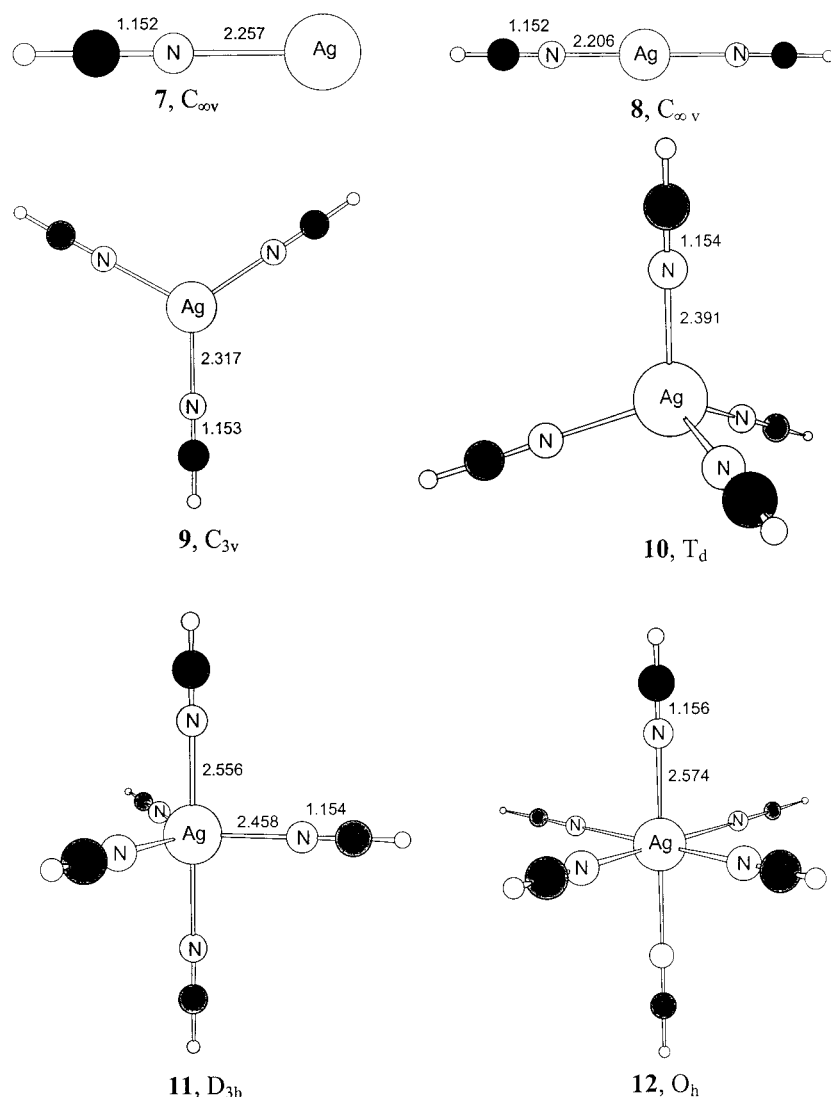


Figure 2. Structures of $\text{Ag}(\text{HCN})_n^+$ ($n = 1-6$) for directly coordinated complexes, as optimized at B3LYP/DZVP. Bond lengths are in Å.

TABLE 2: Enthalpies and Free Energies for Reactions $\text{Ag}(\text{NCX})_n^+ + \text{XCN} \rightarrow \text{Ag}(\text{NCX})_{n+1}^{+a}$

product structure number	$-\Delta H_{\text{un}}(298)$	BSSE	$-\Delta H_{\text{cor}}(298)$	$-\Delta G_{\text{cor}}(298)$
1	42.1	2.0	40.1	33.3
2	37.7	2.4	35.3	27.4
3	17.7	1.8	15.9	9.1
4	12.7	1.9	10.8	3.4
5	5.8	N/A ^b	N/A ^b	-2.7 ^c
6	2.7	N/A ^b	N/A ^b	-2.4 ^c
7	33.2	2.1	31.2	25.6
8	30.9	2.6	28.3	23.8
9	15.7	2.2	13.5	11.8
10	11.9	2.2	9.7	6.7
11	5.7	2.4	3.3	-1.6
12	4.3	2.1	2.2	-2.0

^a X = H or CH₃ and $n = 0-5$. All values are in kcal mol⁻¹.

^b $\Delta G(298)$ is positive without correcting for BSSE. ^c Uncorrected for BSSE.

are given in Table 2. It is apparent that Ag^+ binds tightly only to the first two ligands, with the first addition having a slightly larger binding enthalpy than that of the second. This pattern was also observed for the sequential additions of ammonia to Ag^+ .³⁹ The binding enthalpies with HCN are calculated to be 31.2 and 28.3 kcal mol⁻¹, while those with CH₃CN are 40.1 and 35.3 kcal mol⁻¹ for the first and second additions,

TABLE 3: Threshold Energies, E_0 (eV), for the CID of $\text{Ag}(\text{NCCH}_3)^+$ and $\text{Ag}(\text{NCCH}_3)_2^+$ at 0 K

ion	no RRKM	PSL TS	$\Delta S^{\ddagger a}$	tight TS	ΔS^{\ddagger}
$\text{Ag}(\text{NCCH}_3)^+$	1.68 ± 0.06^b	1.68 ± 0.06	3.0	1.62 ± 0.06	-6.2
$\text{Ag}(\text{NCCH}_3)_2^+$	1.64	1.50	1.6	1.17	-9.4

^a Calculated at 1000 K; in cal K⁻¹ mol⁻¹. ^b Absolute standard deviation; measurements in triplicate.

respectively. The third and fourth ligands in both series are much more weakly bound to the Ag^+ ion, with binding enthalpies of 13.5 and 9.7 kcal mol⁻¹ for HCN and 15.9 and 10.8 kcal mol⁻¹ for CH₃CN, respectively. The fifth and sixth ligands are the least tightly bound with binding enthalpies of only 3–6 kcal mol⁻¹; furthermore, the free energies of the formation reactions are positive, indicating that formation of these adducts is unfavorable.

The results of the threshold CID analyses are provided in Table 3 (Figure 3 shows the threshold curves). Table 3 includes three types of E_0 values: those that do not include the RRKM lifetime analysis (an upper limit to the real thresholds) plus two other types in which lifetime analysis is included. The first of these assumes a PSL TS (lower limit of the kinetic shift), and the second assumes a tight TS (upper limit of the kinetic shift). The relative standard deviation of the threshold of reaction 2 is

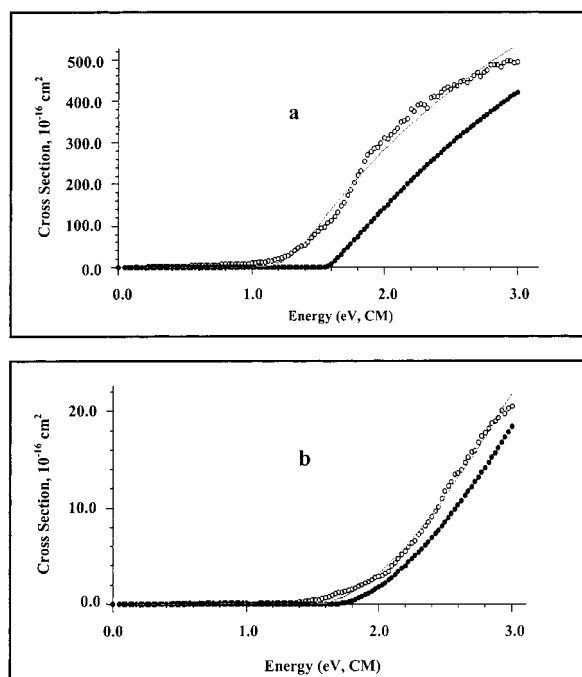


Figure 3. Threshold energy-resolved collision-induced dissociation curves. Open circles: Zero-pressure extrapolated cross sections at 298 K. Solid line: Best fit to the data. Solid circle: Model cross section at 0 K. Panel a: $\text{Ag}(\text{NCCH}_3)_2^+ \rightarrow \text{Ag}(\text{NCCH}_3)^+ + \text{CH}_3\text{CN}$. Panel b: $\text{Ag}(\text{NCCH}_3)^+ \rightarrow \text{Ag}^+ + \text{CH}_3\text{CN}$.

3.6%. While we have not actually measured the uncertainty for the threshold measurement of reaction 4, previous measurements indicate that standard deviations are typically within 5%.⁷⁴

The reactions under consideration are probably best described as simple bond cleavages. Thus, the most accurate E_0 values are expected to be those obtained from the PSL TS model. A comparison of the three E_0 values without RRKM treatment and those obtained with PSL TS treatment shows that the dissociation of the $\text{Ag}(\text{NCCH}_3)^+$ complex exhibits zero kinetic shift, in contrast to that of the $\text{Ag}(\text{NCCH}_3)_2^+$ complex, for which the kinetic shift is approximately 0.14 eV or 3.2 kcal mol⁻¹. The binding enthalpies at 0 K, ΔH_0^0 , of the first and second acetonitrile molecules to Ag^+ , as measured using threshold CID, are 38.7 and 34.6 kcal mol⁻¹, respectively. The corresponding ΔH_{298}^0 values, after addition of the appropriate thermal energies (Table 1), are 39.4 and 34.7 kcal mol⁻¹. The DFT values are higher, but are both within 0.7 kcal mol⁻¹ of the experimental values.

The binding enthalpies for the addition of two CH_3CN molecules to the silver (I) ion are 75.4 and 74.1 kcal mol⁻¹ from DFT calculations and threshold CID measurements, respectively. These values compare more favorably with Deng and Kebarle's experimental value⁴² of 84.3 ± 3 kcal mol⁻¹ than with the theoretical value of 48.6 kcal mol⁻¹ given by Tsutsui et al.⁵⁵ for this reaction. In addition, it is noteworthy that the calculated enthalpies for the reactions of $\text{Ag}(\text{NH}_3)^+$, $\text{Ag}(\text{NH}_3)_2^+$, and $\text{Ag}(\text{NH}_3)_3^+$ with NH_3 ,³⁹ using the same level of theory as in that the current work, are all in good agreement with Holland and Castleman's⁷⁵ experimentally determined ΔH_{298}^0 values for these reactions. Summing the calculated value of 40.1 kcal mol⁻¹ for the first addition of NH_3 to Ag^+ with Castleman's experimental value of 36.8 kcal mol⁻¹ for the second addition, we obtain 76.9 kcal mol⁻¹ for the combined reaction. This is lower than the value of 85.6 kcal mol⁻¹ given by Kebarle for this reaction by 8.7 kcal mol⁻¹. The difference between our

TABLE 4: Total Electronic, Unscaled Zero-Point, and Thermal Energies as well as Entropies for Ligands XCN Calculated at B3LYP/DZVP

X group	energy (Hartrees)	ZPE (kcal mol ⁻¹)	$H_{298}^0 - H_0^0$ (kcal mol ⁻¹)	entropy (cal K ⁻¹ mol ⁻¹)
<i>p</i> -C ₆ H ₄ N(CH ₃) ₂	-458.50181	108.0	7.3	102.0
<i>p</i> -C ₆ H ₄ NH ₂	-379.88348	72.5	5.4	85.2
N(CH ₃) ₂	-227.42580	57.2	4.4	75.8
NH ₂	-148.80158	21.4	2.8	59.2
C ₆ H ₅	-324.51672	62.1	4.5	78.7
OH	-168.66011	13.4	2.7	57.8
F	-192.66838	6.3	2.4	53.6
CN	-185.67038	10.2	3.0	57.6
CF ₃	-430.53807	14.1	3.8	73.6
<i>p</i> -C ₆ H ₄ NO ₂	-529.05103	63.6	6.0	93.2
NO ₂	-297.93309	12.4	3.3	68.6

TABLE 5: Total Electronic, Unscaled Zero-Point, and Thermal Energies as well as Entropies for AgNCX⁺ Complexes Calculated at B3LYP/DZVP

X group	energy (Hartrees)	ZPE (kcal mol ⁻¹)	$H_{298}^0 - H_0^0$ (kcal mol ⁻¹)	entropy (cal K ⁻¹ mol ⁻¹)
<i>p</i> -C ₆ H ₄ N(CH ₃) ₂	-5657.78585	108.9	8.6	121.1
<i>p</i> -C ₆ H ₄ NH ₂	-5579.16389	72.8	7.0	105.2
N(CH ₃) ₂	-5426.70426	57.9	5.9	95.8
NH ₂	-5348.07200	21.6	4.3	78.4
C ₆ H ₅	-5523.78747	62.8	5.8	95.1
OH	-5367.92225	14.1	3.0	75.2
F	-5391.91700	7.2	3.7	71.0
CN	-5384.90855	10.6	4.2	74.0
CF ₃	-5629.77974	14.6	5.2	89.5
<i>p</i> -C ₆ H ₄ NO ₂	-5728.30985	64.1	7.4	110.2
NO ₂	-5497.16814	12.7	4.7	86.9

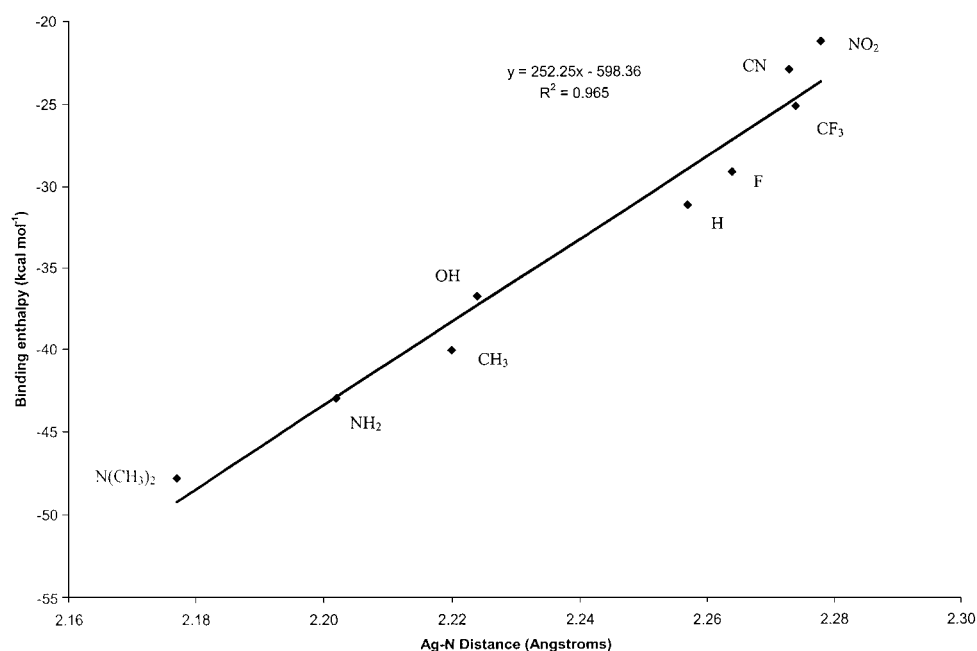
DFT and Kebarle's experimentally determined binding enthalpy for the addition of two CH_3CN molecules to Ag^+ ($84.3 - 75.4 = 8.9$ kcal mol⁻¹) is virtually identical to that for two NH_3 molecules. This suggests a systematic difference in the Ag^+ binding enthalpies by about 9 kcal mol⁻¹ between our DFT data and the equilibrium data of Deng and Kebarle.⁴² Our threshold CID result for the accumulative binding of two CH_3CN molecules is 1.3 kcal mol⁻¹ lower than our DFT number.

Ligand Substituent Effects. The effects of varying the X group in the reaction $\text{Ag}^+ + \text{N}\equiv\text{C}-\text{X} \rightarrow \text{Ag}-\text{N}\equiv\text{C}-\text{X}^+$ on the reaction enthalpy was investigated. The total electronic, unscaled zero-point, and thermal energies and the entropies of all $\text{N}\equiv\text{C}-\text{X}$ and $\text{Ag}-\text{N}\equiv\text{C}-\text{X}^+$ species investigated are given in Tables 4 and 5. The silver (I) ion binding enthalpies of the various adducts, given in Table 6, range from 52.2 kcal mol⁻¹ for X = *p*-C₆H₄N(CH₃)₂ to 21.3 kcal mol⁻¹ for X = NO₂. As the binding enthalpy decreases, there is a concomitant increase in the silver nitrogen bond distance. There are linear relationships between the Ag-N distances and the binding energies for both the aliphatic and aromatic nitrile complexes studied here (see Figures 4 and 5). A correlation between the silver (I) ion affinities and the proton affinities of all ligands in this study is also evident (see Figure 6).

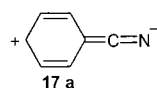
Structural Parameters in Cyanobenzenes. The cyano group functions as an electron-withdrawing group in cyanobenzene. This is reflected in the bond lengths given in Figure 7. The C-N distance of 1.166 Å in cyanobenzene is slightly longer than that in HCN (1.160 Å), and there is an alternation of bond lengths in the phenyl ring with the C₁-C₂, C₁-C₆, C₃-C₄, and C₄-C₅ distances all being slightly longer than those calculated at the same level of theory for benzene (1.401 Å), while the C₂-C₃ and C₅-C₆ distances are shorter at 1.395 Å. All these

TABLE 6: Enthalpies and Free Energies for Reactions $\text{Ag}^+ + \text{XCN} \rightarrow \text{Ag}(\text{NCX})^+$

X group	site of Ag^+ attachment	$-\Delta H_{\text{un}}(298)$	BSSE	$-\Delta H_{\text{cor}}(298)$	$-\Delta G_{\text{cor}}(298)$
$p\text{-C}_6\text{H}_4\text{N}(\text{CH}_3)_2$	Cyano	53.9	1.7	52.2	45.2
	Amino	32.4	—	—	24.7 ^a
$p\text{-C}_6\text{H}_4\text{NH}_2$	Cyano	51.2	1.8	49.4	43.5
	Amino	30.7	—	—	23.3 ^a
$\text{N}(\text{CH}_3)_2$	Cyano	49.7	1.9	47.8	41.8
	Amino	22.0	—	—	14.3 ^a
C_6H_5	Cyano	45.0	1.8	43.2	37.2
	NH ₂	45.1	2.1	43.0	36.8
OH	Amino	18.8	—	—	11.8 ^a
	Cyano	38.8	2.0	36.8	30.1
$p\text{-C}_6\text{H}_4\text{NO}_2$	Hydroxy	8.5	—	—	2.4 ^a
	Cyano	37.6	1.8	35.9	29.1
F	Nitro	36.0	—	—	28.9 ^a
	Cyano	31.0	1.8	29.2	22.5
CF_3	Cyano	26.9	1.7	25.2	18.0
	Trifluoromethyl	5.7	—	—	0.1 ^a
CN	Cyano	25.0	2.0	23.0	16.0
NO_2	Cyano	22.9	1.6	21.3	14.9
	Nitro	15.6	—	—	8.2 ^a

^a Values are uncorrected for BSSE.**Figure 4.** Silver (I) ion binding enthalpy plotted against the silver nitrogen distance in all aliphatic $\text{X}-\text{C}\equiv\text{N}$ ligands. In all cases, the site of Ag^+ attachment is to the cyano nitrogen.

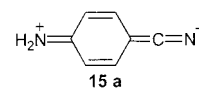
geometric changes are consistent with a minor contribution from resonance structure **17a**.



Coordination of Ag^+ to the nitrogen of cyanobenzene converts the substituent into a stronger electron-withdrawing group, and the geometric trends in bond lengths in the phenyl ring caused by substitution by CN are in the same direction but more pronounced. The largest geometric change resulting from the addition of Ag^+ is in the $\text{Ph}-\text{CN}$ bond, where there is a decrease of 0.015 Å.

Introduction of a $p\text{-NH}_2$ group into cyanobenzene assists in the donation of electron density to the cyano group from the phenyl ring, and the C_3-C_4 and C_4-C_5 bonds in $p\text{-NH}_2\text{PhCN}$ are both lengthened by 0.011 Å relative to those in PhCN . The

effects of the $p\text{-NH}_2$ group on the other bonds within the ring are less pronounced but favor a larger contribution from the resonance structure **15a**. Addition of Ag^+ to the N of CN group has larger effects on the geometry of the ring, changes that further indicate the importance of resonance structure **15a**.



The $p\text{-NO}_2$ group is electron withdrawing and has a much smaller effect than the $p\text{-NH}_2$ group on the structure of the ring. The addition of Ag^+ to the cyano group of $p\text{-NO}_2\text{PhCN}$ results in changes almost identical to those that occur with the addition of Ag^+ to PhCN .

Linear Free Energy Relationships. The Ag^+ affinities of substituted cyanobenzenes span a small range from 35.9 kcal mol^{-1} for the $p\text{-NO}_2$ substituted to 52.2 kcal mol^{-1} for the

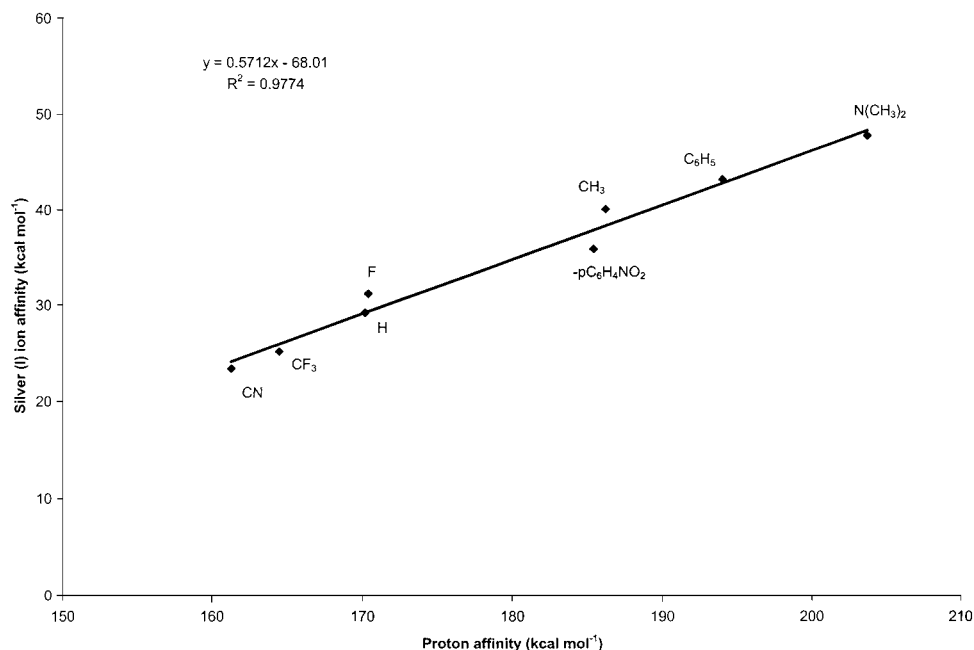


Figure 5. Silver (I) ion binding enthalpy plotted against the silver nitrogen distance in all aromatic $X-C\equiv N$ ligands. In all cases, the site of Ag^+ attachment is to the cyano nitrogen.

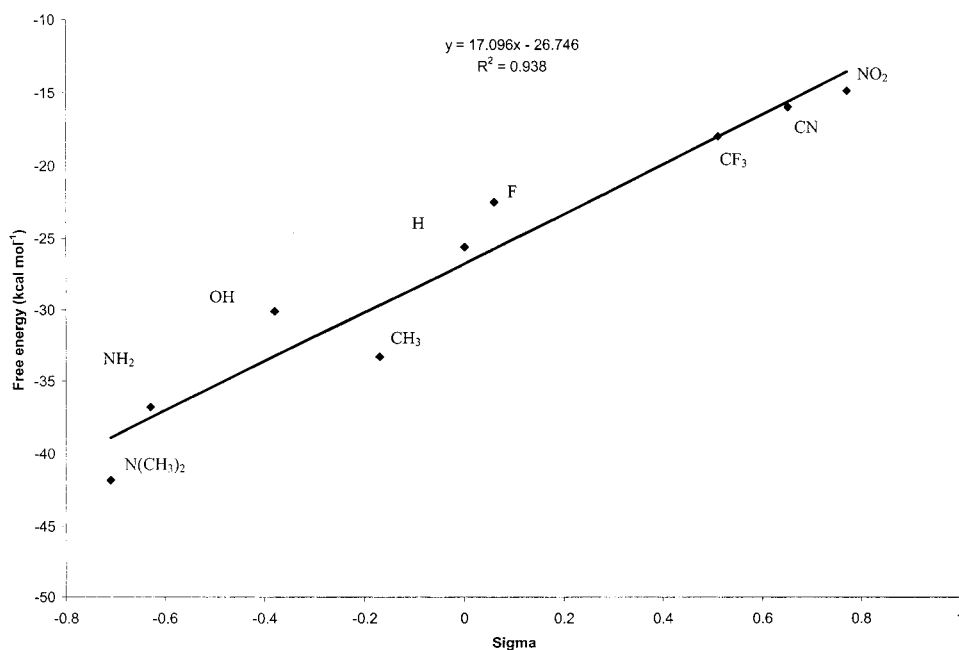


Figure 6. Silver (I) ion affinities plotted against proton affinities for $X-C\equiv N$ ligands. In all cases, the ion attachment is to the cyano nitrogen.

p - $N(CH_3)_2$ substituted. The calculated free energies of formation plotted against the Hammett σ_p substituent constants^{76,77} for the limited number of cyanobenzenes studied here show a linear correlation with a ρ value of 10.6 (Figure 8).

The cyano complexes essentially involve donation from the lone pair electrons of σ -symmetry, formally localized on the N, to Ag^+ , and there is little π -interaction between the filled d-orbitals on Ag^+ and the filled π -orbitals of the cyano group. In this sense, the interactions between Ag^+ and the substituents, X, in aliphatic complexes $Ag-N\equiv CX^+$ are not too dissimilar from those between these substituents and the carboxylic acid group in the benzoic acids, the class of compounds upon which the Hammett substituent constants are based. We therefore plotted the calculated free energies for the binding of Ag^+ in all aliphatic complexes against the Hammett σ_p substituent

constants for their respective X groups and obtained the linear plot shown in Figure 9. The slope of this plot, ρ , is 17.1. This value is larger than that for the p -substituted cyanobenzenes, reflecting both the closer proximity of the substituent to the site of silver (I) ion attachment and the larger dependence on the substituent for charge delocalization in the smaller aliphatic ions.

Alternative Sites of Ag (I) Ion Addition. Alternative sites to the cyano nitrogen for silver (I) ion binding were explored. The interaction of Ag^+ to benzene has been investigated by many groups,^{78–80} and a binding energy was recently calculated to be $35.4 \text{ kcal mol}^{-1}$,⁷⁹ while experimental values of 37 ± 2 and 35 kcal mol^{-1} were reported.⁷⁹ The only other possible π -complex that could form with any of these ligands is from the interaction of Ag^+ with the triple bond of the cyano group.

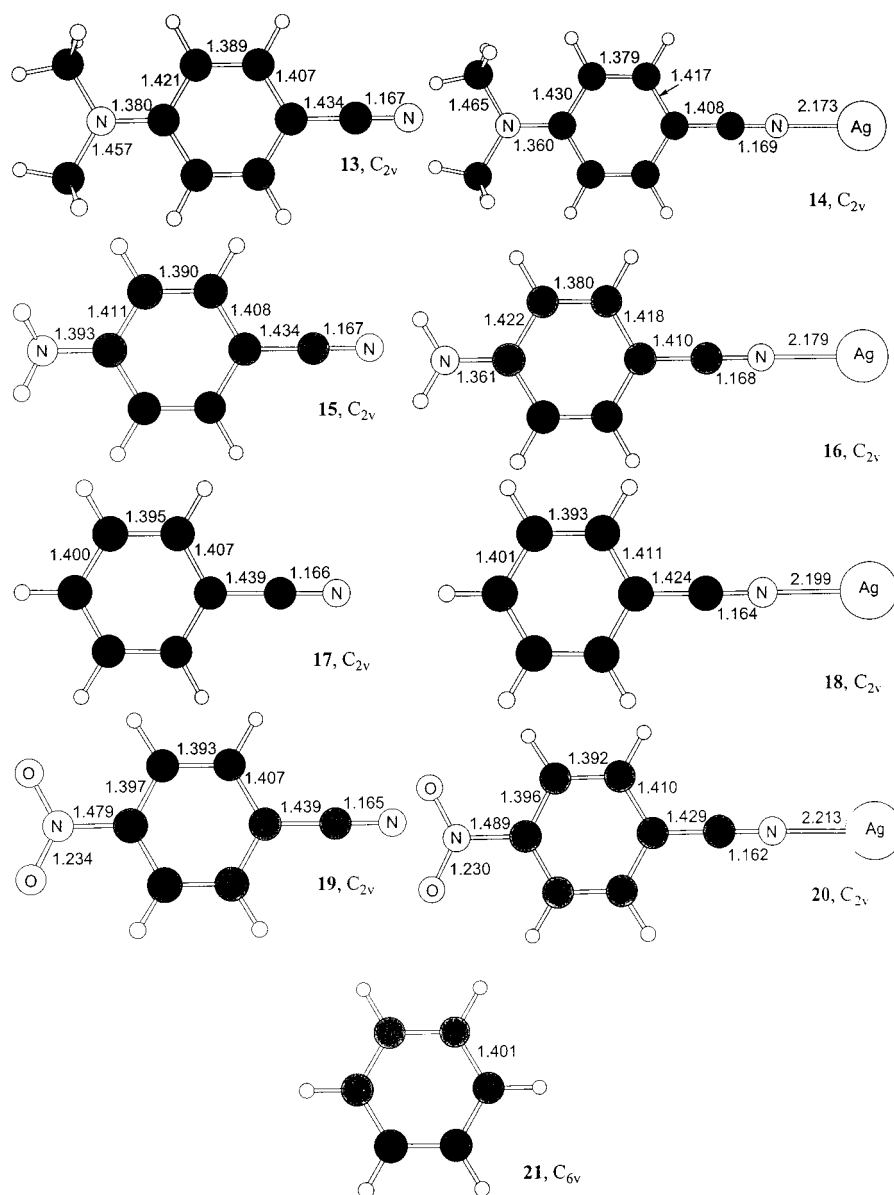


Figure 7. Structures of aromatic ligands, $X-p-C_6H_4C\equiv N$ and $Ag^+-X-p-C_6H_4C\equiv N$, and C_6H_6 . All structures are optimized at B3LYP/DZVP. Bond lengths are in Å.

For all the ligands under study here, no such π -complexes were found to exist at minima.

Other possible σ -complexes were also investigated. The enthalpies and free energies of silver (I) ion binding in these σ -complexes are shown in Table 5. These results indicate that Ag^+ attachment to the cyano nitrogen is always the favored site of binding. In the case of $p-NCC_6H_4NO_2$ the dicoordination of silver (I) to the oxygen atoms of the NO_2 group has a binding enthalpy of 36.0 kcal mol $^{-1}$, which is comparable to, but still lower than, that for silver (I) addition to the cyano nitrogen.

Conclusions

Here we have investigated the electronic structures and binding energies of $Ag(NCCH_3)_n^+$ and $Ag(NCH)_n^+$ complexes, where $n = 1-6$. Molecular orbital calculations indicate that formation of these complexes where the ligands are directly coordinated to the central silver ion with values of $n \leq 4$ should occur in the gas phase at 298 K. However, the free energies for formation of the four-coordinate species are very small.

Experimental binding energies for the first and second addition of CH_3CN molecules to Ag^+ were determined by means of the threshold method and were found to be in good agreement with those obtained from B3LYP/DZVP calculations.

We have addressed the considerable disagreement between Tsutsui et al.⁵⁵ and Deng and Kebarle⁴² for the addition of two CH_3CN molecules to Ag^+ . On the basis of the theoretical and experimental evidence presented here, it is clear that the theoretical approach adopted by Tsutsui et al.⁵⁵ severely underestimates the binding energies of these reactions, almost by a factor of 2.

The effects of varying the substituent X on the enthalpy of the reaction $Ag^+ + N\equiv C-X \rightarrow Ag-N\equiv C-X^+$ was also investigated. Positive correlations were shown to exist between the binding enthalpies and the $Ag-N$ distances, as well as between the silver ion affinities and the proton affinities for all the ligands $N\equiv C-X$ examined.

Finally, the plots of the Ag^+ binding free energies against the Hammett σ_p substituent constants were shown to give linear

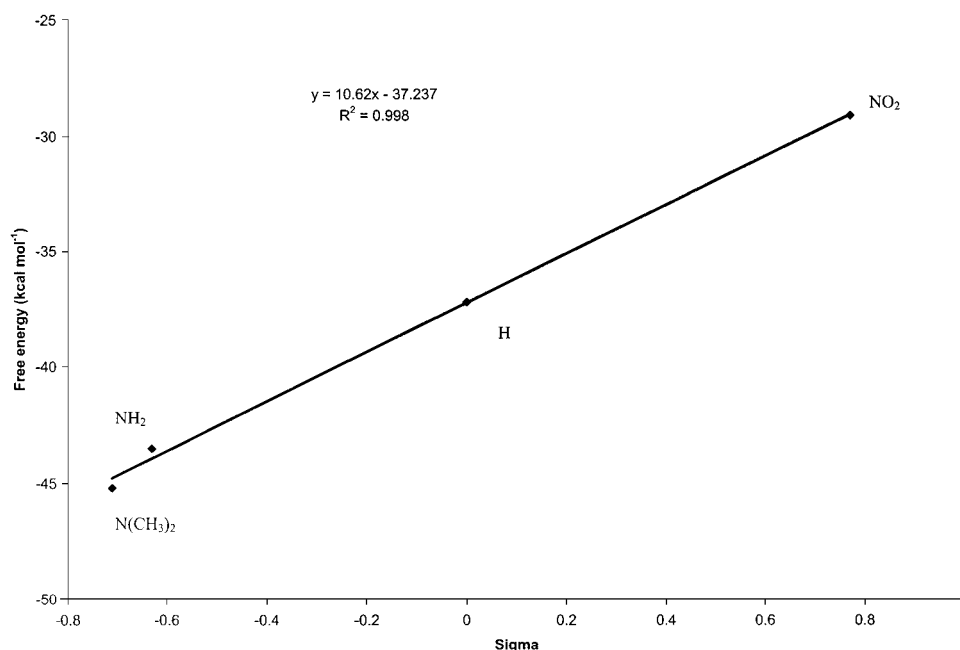


Figure 8. Free energies for silver (I) ion binding to aromatic ligands, $X-p-C_6H_4C\equiv N$, plotted against Hammett's σ_p substituent constants.

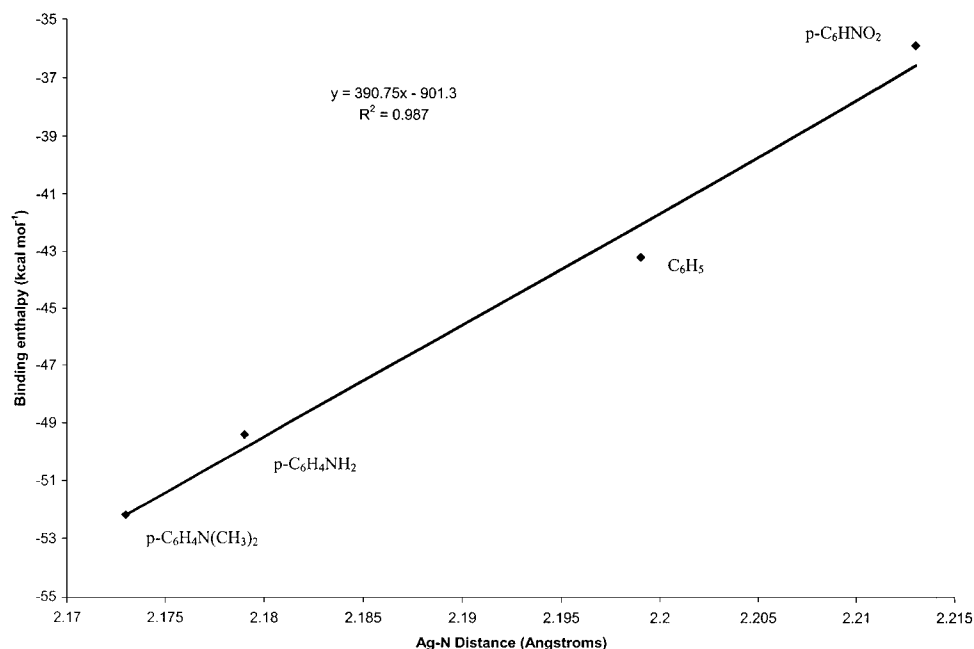


Figure 9. Free energies for silver (I) ion binding aliphatic ligands, $X-C\equiv N$, plotted against Hammett's σ_p substituent constants.

correlations for both aromatic and aliphatic ligands studied with the ρ values being 10.6 and 17.1, respectively. The larger ρ value for the aliphatic ligands reflects both the closer proximity of the substituent to the site of silver ion attachment and the larger dependence on the substituent for charge delocalization in the smaller aliphatic ions.

Acknowledgment. We thank the Natural Sciences and Engineering Research Council of Canada (NSERC), MDS SCIEX, Canadian Foundation for Innovation (CFI), and the Ontario Innovation Trust (OIT) for their continued financial support. Steve Quan's technical assistance is gratefully acknowledged. The authors are indebted to Professor P. B. Armentrout for making the CRUNCH program available to them. T.S. acknowledges financial support by an Ontario Graduate Scholarship in Science and Technology.

Supporting Information Available: Vibrational frequencies and rotational constants provided by the DFT hybrid method at the B3LYP/DZVP level of theory for both the silver complex ions and the dissociation products. This material is available free of charge via the Internet at <http://pubs.acs.org>.

References and Notes

- (1) Sauer, J. *Chem. Rev.* **1989**, 89, 199.
- (2) Backvall, J.-E.; Bokman, F.; Blomberg, M. R. A. *J. Am. Chem. Soc.* **1992**, 114, 534.
- (3) Dougherty, D. A. *Science* **1996**, 271, 163.
- (4) Szilagy, R. K.; Frenking, G. *Organometallics* **1997**, 16, 4807.
- (5) Bene, J. E. D. *J. Phys. Chem.* **1996**, 100, 6284.
- (6) Feller, D.; Glendening, E. D.; Kendall, R. A.; Peterson, K. A. *J. Chem. Phys.* **1994**, 100, 4981.
- (7) Glendening, E. D.; Feller, D. *J. Phys. Chem.* **1995**, 99, 3060.
- (8) Glendening, E. D. *J. Am. Chem. Soc.* **1996**, 118, 2473.

- (9) Feller, D.; Glendening, E. D.; Woon, D. E.; Feyereisen, M. W. *J. Chem. Phys.* **1995**, *103*, 3526.
- (10) Magnusson, E. *J. Comput. Chem.* **1994**, *16*, 1027.
- (11) Periole, X.; Allouche, D.; Daudey, J.-P.; Sanejouand, Y.-H. *J. Phys. Chem. B* **1997**, *101*, 5018.
- (12) Hoyau, S.; Ohanessian, G. *Chem. Phys. Lett.* **1997**, *280*, 266.
- (13) Hoyau, S.; Ohanessian, G. *J. Am. Chem. Soc.* **1997**, *119*, 2016.
- (14) Bowmaker, G. A.; Pabst, M.; Rösch, N.; Schmidbaur, H. *Inorg. Chem.* **1993**, *32*, 880.
- (15) Re, N.; Rosi, M.; Sgamellotti, A.; Floriani, C.; Solari, E. *THEOCHEM* **1993**, *284*, 95.
- (16) El-Nahas, A. M.; Tajina, N.; Hirao, K. *THEOCHEM* **1999**, *469*, 201.
- (17) Luna, A.; Amekraz, B.; Tortajada, J. *Chem. Phys. Lett.* **1997**, *266*, 31.
- (18) Bauschlicher, C. W., Jr.; Langhoff, S. R.; Partridge, H. *J. Chem. Phys.* **1991**, *94*, 2068.
- (19) Bauschlicher, C. W., Jr.; Langhoff, S. R.; Partridge, H. *J. Chem. Phys.* **1991**, *95*, 5142.
- (20) Langhoff, S. R.; Bauschlicher, C. W., Jr.; Partridge, H.; Sodupe, M. *J. Phys. Chem.* **1991**, *95*, 10677.
- (21) Rosi, M.; Bauschlicher, C. W., Jr. *J. Chem. Phys.* **1990**, *92*, 1876.
- (22) Schneider, W. F.; Hass, K. C.; Ramprasad, R.; Adams, J. B. *J. Phys. Chem.* **1996**, *100*, 6032.
- (23) Pavlov, M.; Siegbahn, P. E. M.; Sandström, M. *J. Phys. Chem. A* **1998**, *102*, 219.
- (24) Pople, J. A.; Luke, B. T.; Frisch, M. J.; Binkley, J. S. *J. Phys. Chem.* **1985**, *89*, 2198.
- (25) Pople, J. A.; Curtiss, L. A. *J. Phys. Chem.* **1987**, *91*, 155.
- (26) Pople, J. A.; Curtiss, L. A. *J. Phys. Chem.* **1987**, *91*, 3637.
- (27) Curtiss, L. A.; Raghavachari, K.; Pople, J. A. *Chem. Phys. Lett.* **1993**, *214*, 183.
- (28) Milburn, R. K.; Rodriguez, C. F.; Hopkinson, A. C. *J. Phys. Chem. B* **1997**, *101*, 1837.
- (29) Milburn, R. K.; Baranov, V.; Hopkinson, A. C.; Bohme, D. K. *J. Phys. Chem. A* **1999**, *103*, 6373.
- (30) Ling, Y.; Milburn, R. K.; Hopkinson, A. C.; Bohme, D. K. *J. Am. Soc. Mass Spectrom.* **1999**, *10*, 848.
- (31) Rodriguez, C. F.; Shoeib, T.; Chu, I. K.; Siu, K. W. M.; Hopkinson, A. C. *J. Phys. Chem. A* **2000**, *104*, 5335.
- (32) Rodgers, M. T.; Armentrout, P. B. *J. Phys. Chem. A* **1997**, *101*, 2614.
- (33) Martinho-Simoes, J. A.; Beauchamp, J. L. *Chem. Rev.* **1990**, *90*, 629.
- (34) Freiser, B. S. *Acc. Chem. Res.* **1994**, *27*, 353.
- (35) Freiser, B. S. *J. Mass Spectrom.* **1996**, *31*, 703.
- (36) Bauschlicher, C. W., Jr.; Partridge, H. *J. Phys. Chem.* **1991**, *95*, 3946.
- (37) Bauschlicher, C. W., Jr.; Partridge, H. *Chem. Phys. Lett.* **1991**, *181*, 129.
- (38) Bauschlicher, C. W., Jr.; Partridge, H. *J. Phys. Chem.* **1991**, *95*, 9694.
- (39) Shoeib, T.; Milburn, R. K.; Koyanagi, G. K.; Lavrov, V. V.; Bohme, D. K.; Siu, K. W. M.; Hopkinson, A. C. *Int. J. Mass Spectrom.* **2000**, *201*, 87.
- (40) Narula, S. S.; Mehra, R. K.; Winge, D. R.; Armitage, I. M. *J. Am. Chem. Soc.* **1991**, *113*, 9354.
- (41) Stillman, M. J.; Presta, A.; Gui, Z.; Jiang, D.-T. In *Metal-Based Drugs*; Gielen, M., Ed.; Freund: London, 1994; Vol. 1, p 375.
- (42) Deng, H.; Kebarle, P. *J. Phys. Chem. A* **1998**, *102*, 571.
- (43) Li, H.; Siu, K. W. M.; Guevremont, R.; Le Blanc, J. C. Y. *J. Am. Soc. Mass Spectrom.* **1997**, *8*, 781.
- (44) Li, H.; Lee, V. W.-M.; Lau, T.-C.; Guevremont, R.; Siu, K. W. M. *J. Am. Soc. Mass Spectrom.* **1998**, *9*, 766.
- (45) Lee, V. W.-M.; Li, H.; Lau, T.-C.; Siu, K. W. M. *J. Am. Chem. Soc.* **1998**, *120*, 7302.
- (46) Chu, I. K.; Guo, X.; Lau, T.-C.; Siu, K. W. M. *Anal. Chem.* **1999**, *71*, 2364.
- (47) Chu, I. K.; Shoeib, T.; Guo, X.; Rodriguez, C. F.; Lau, T.-C.; Hopkinson, A. C.; Siu, K. W. M. *J. Am. Soc. Mass Spectrom.* in press.
- (48) Yamaguchi, T.; Lindqvist, O. *Acta Chem. Scand.* **1983**, *A37*, 685.
- (49) Antti, C.-J.; Lundberg, B. K. S. *Acta Chem. Scand.* **1971**, *25*, 1758.
- (50) Dyason, J. C.; Healy, P. C.; Engelhardt, L. M.; White, A. H. *Aust. J. Chem.* **1985**, *38*, 1325.
- (51) Nilsson, K.; Oskarsson, A. *Acta Chem. Scand.* **1984**, *A38*, 79.
- (52) Goodwin, K. V.; McMillin, D. R.; Robinson, W. R. *Inorg. Chem.* **1986**, *25*, 2033.
- (53) Bjerrum, J. *Acta Chem. Scand.* **1986**, *A40*, 392.
- (54) Carlucci, L.; Ciani, G.; Proserpio, D. M.; Sironi, A. *J. Am. Chem. Soc.* **1995**, *117*, 4562.
- (55) Tsutsui, Y.; Sugimoto, K.-I.; Wasada, H.; Inada, Y.; Funahashi, S. *J. Phys. Chem. A* **1997**, *101*, 2900.
- (56) Frisch, M. J.; Trucks, G. W.; Schlegel, H. B.; Scuseria, G. E.; Robb, M. A.; Cheeseman, J. R.; Zakrewski, V. G.; Montgomery, J. A., Jr.; Stratmann, R. E.; Burant, J. C.; Dapprich, S.; Millam, J. M.; Daniels, A. D.; Rudin, K. N.; Strain, M. C.; Farkas, O.; Tomasi, J.; Barone, V.; Cossi, M.; Cammi, R.; Mennucci, B.; Pomelli, C.; Adamo, C.; Clifford, S.; Ochterski, J.; Petersson, G. A.; Ayala, P. Y.; Cui, Q.; Morokuma, K.; Malick, D. K.; Rabuck, A. D.; Raghavachari, K.; Foresman, J. B.; Cioslowski, J.; Ortiz, J. V.; Stefanov, B. B.; Liu, G.; Liashenko, A.; Piskorz, P.; Komaromi, I.; Gomperts, R.; Martin, R. L.; Fox, D. J.; Keith, T.; Al-Laham, M. A.; Peng, C. Y.; Nanayakkara, A.; Gonzalez, C.; Challacombe, M.; Gill, P. M. W.; Johnson, B.; Chen, W.; Wong, M. W.; Andres, J. L.; Gonzalez, C.; Head-Gordon, M.; Replogle, E. S.; Pople, J. A. *Gaussian 98*, Revision A.5; Gaussian Inc.: Pittsburgh, PA, 1998.
- (57) Becke, A. D. *Phys. Rev.* **1988**, *A38*, 3098.
- (58) Becke, A. D. *J. Chem. Phys.* **1993**, *98*, 5648.
- (59) Lee, C.; Yang, W.; Parr, R. G. *Phys. Rev.* **1988**, *B37*, 785.
- (60) Godbout, N.; Salahub, D. R.; Andzelm, J.; Wimmer, E. *Can. J. Chem.* **1992**, *70*, 560.
- (61) Godbout, N. *Ensemble de base pour la théorie de la fonctionnelle de la densité - Structures moléculaires, propriétés mono-électroniques et modèles de zéolites*. Ph.D. Thesis, Université de Montréal, Montréal, Canada, 1996.
- (62) Boys, S. F.; Bernardi, F. *Mol. Phys.* **1970**, *19*, 553.
- (63) Ervin, K. M.; Armentrout, P. B. *J. Chem. Phys.* **1985**, *83*, 166.
- (64) Weber, M. E.; Elkind, J. L.; Armentrout, P. B. *J. Chem. Phys.* **1986**, *84*, 1521.
- (65) Schultz, R. H.; Crellin, K. C.; Armentrout, P. B. *J. Am. Chem. Soc.* **1991**, *113*, 8590.
- (66) Dalleska, N. F.; Honma, K.; Sunderlin, L. S.; Armentrout, P. B. *J. Am. Chem. Soc.* **1994**, *116*, 3519.
- (67) Shvartsburg, A. A.; Ervin, K. M.; Frederick, J. H. *J. Chem. Phys.* **1996**, *104*, 8458.
- (68) Rodgers, M. T.; Ervin, K. M.; Armentrout, P. B. *J. Chem. Phys.* **1997**, *106*, 4499.
- (69) Rodgers, M. T.; Armentrout, P. B. *J. Chem. Phys.* **1998**, *109*, 1787.
- (70) Dawson, P. H.; French, J. B.; Buckley, J. A.; Douglas, D. J.; Simmons, D. *Org. Mass Spectrom.* **1982**, *17*, 205.
- (71) Gilbert, R. G.; Smith, S. C. *Theory of Unimolecular and Recombination Reactions*; Blackwell Scientific Publications: Oxford, 1990.
- (72) Truhlar, D. G.; Garrett, B. C.; Klippenstein, S. J. *J. Phys. Chem.* **1996**, *100*, 12771.
- (73) Holbrook, K. A.; Pilling, M. J.; Robertson, S. H. *Unimolecular Reactions*, 2nd ed.; Wiley: New York, 1996.
- (74) El Aribi, H.; Shoeib, T.; Ling, Y.; Hopkinson, A. C.; Siu, K. W. M. Proceedings of the 48th ASMS Conference on Mass Spectrometry, Long Beach, CA, June 11–15, 2000 (ASMS web page. <http://www.asms.org>).
- (75) Holland, P. M.; Castleman, A. W., Jr. *J. Chem. Phys.* **1982**, *76*, 4195.
- (76) Hammett, L. P. *Chem. Rev.* **1935**, *17*, 125.
- (77) Ehrenson, S.; Brownlee, R. T. C.; Taft, R. W. *Prog. Phys. Org. Chem.* **1973**, *10*.
- (78) Ho, Y.-P.; Yang, Y.-C.; Klippenstein, S. J.; Dunbar, R. C. *J. Phys. Chem. A* **1997**, *101*, 3338.
- (79) Ma, N. L.; Ng, K. M.; Tsang, C. W. *Chem. Phys. Lett.* **1997**, *277*, 306.
- (80) Bauschlicher, C. W., Jr.; Partridge, H.; Langhoff, S. R. *J. Phys. Chem.* **1992**, *96*, 3273.